MOLECULAR AND CELLULAR BIOLOGY, Feb. 1998, p. 665–675 Vol. 18, No. 2
0270-7306/98/$04.00+0

RNA Polymerase I-Promoted *HIS4* Expression Yields Uncapped, Polyadenylated mRNA That Is Unstable and Inefficiently Translated in *Saccharomyces cerevisiae*

HSIU-JUNG LO,† HAN-KUEI HUANG, AND THOMAS F. DONAHUE*

Department of Biology, Indiana University, Bloomington, Indiana 47405

Received 28 March 1997/Returned for modification 8 May 1997/Accepted 6 November 1997

The *HIS4* gene in *Saccharomyces cerevisiae* was put under the transcriptional control of RNA polymerase I to determine the in vivo consequences on mRNA processing and gene expression. This gene, referred to as *rhis4*, was substituted for the normal *HIS4* gene on chromosome III. The *rhis4* gene transcribes two mRNAs, of which each initiates at the polymerase (pol) I transcription initiation site. One transcript, *rhis4s*, is similar in size to the wild-type *HIS4* mRNA. Its 3′ end maps to the *HIS4* 3′ noncoding region, and it is polyadenylated. The second transcript, *rhis4l*, is bicistronic. It encodes the *HIS4* coding region and a second open reading frame, *YCL184*, that is located downstream of the *HIS4* gene and is predicted to be transcribed in the same direction as *HIS4* on chromosome III. The 3′ end of *rhis4l* maps to the predicted 3′ end of the *YCL184* gene and is also polyadenylated. Based on in vivo labeling experiments, the *rhis4* gene appears to be more actively transcribed than the wild-type *HIS4* gene despite the near equivalence of the steady-state levels of mRNAs produced from each gene. This finding indicated that *rhis4* mRNAs are rapidly degraded, presumably due to the lack of a cap structure at the 5′ end of the mRNA. Consistent with this interpretation, a mutant form of *XRN1*, which encodes a 5′-3′ exonuclease, was identified as an extragenic suppressor that increases the half-life of *rhis4* mRNA, leading to a 10-fold increase in steady-state mRNA levels compared to the wild-type *HIS4* mRNA level. This increase is dependent on pol I transcription. Immunoprecipitation by anticap antiserum suggests that the majority of *rhis4* mRNA produced is capless. In addition, we quantitated the level of His4 protein in a *rhis4 xrn1*Δ genetic background. This analysis indicates that capless mRNA is translated at less than 10% of the level of translation of capped *HIS4* mRNA. Our data indicate that polyadenylation of mRNA in yeast occurs despite *HIS4* being transcribed by RNA polymerase I, and the 5′ cap confers stability to mRNA and affords the ability of mRNA to be translated efficiently in vivo.

RNA transcribed by RNA polymerase (pol) II undergoes a number of covalent modifications before being exported to the cytoplasm as mature mRNA and subsequently translated. Two such modifications, capping at the 5′ end and polyadenylation at the 3′ end of mRNA, are believed to be limited to the RNA pol II transcriptional machinery. The addition of the unique cap structure to the 5′ end of all mature eukaryotic mRNAs is tightly coupled to RNA pol II transcription as the cap can be detected when the 5′ end of mRNA emerges from the pol II transcriptional machinery (22, 32, 49). It has been shown that the cap structure is important for RNA transport, pre-RNA splicing, and mRNA stability (16, 23, 30, 40).

One of the best-understood functions of the cap structure is its role in translation initiation. According to the ribosomal scanning model (34), the eukaryotic initiation factor eIF-4F complex is required for the binding of the ribosomal preinitiation complex to mRNAs and for unwinding secondary structure in the 5′ leader region. This allows the preinitiation complex to scan for the first downstream AUG start codon in a 5′-to-3′ direction (for reviews, see references 25 and 54). The well-accepted ribosomal scanning model (cap-dependent initiation mechanism) accounts for most of eukaryotic translation initiation events. However, a number of mRNAs have been described to be translated by a cap-independent mechanism of translation. For example, upon poliovirus infection of mammalian cells, the eIF-4F initiation complex is rendered nonfunctional as a result of proteolytic cleavage of the p220 subunit. This results in the shutdown of cap-dependent protein synthesis in host cells and allows preferential translation of uncapped viral mRNAs, which occurs by a cap-independent mechanism (reviewed by Sonenberg [55]). Cap-independent translation initiation has also been described for cellular mRNAs (38, 45). Previous studies have used in vivo-expressed capless mRNAs in mammalian cells to investigate the relationship between the cap structure and the translation efficiency (19, 20). However, these studies differ in conclusion as to whether a cap is needed for translation in these cells.

The poly(A) tail at the 3′ end of eukaryotic mRNAs is another distinct feature of eukaryotic mRNAs. The polyadenylation step takes place in the nuclei posttranscriptionally. In short, the AAUAAA- and G/U-rich elements at the 3′ end of mRNA signal transcription termination and specific cleavage followed by consecutive addition of adenosine residues (8, 39, 58). McCracken et al. (39) have reported that the carboxy-terminal domain (CTD) of the pol II large subunit is required for efficient cleavage at the poly(A) site in vivo and that the CTD might associate with CPSF (cleavage and polyadenylation specificity factors) and CstF (cleavage stimulation factors) but not poly(A) polymerase (39), suggesting that the polyadenylation machinery, in part, associates with the pol II transcriptional apparatus. The synthesized tail is typically homogeneous in length, ranging from 75 nucleotides (nt) (40) in yeast cells to 200 nt (3) in mammalian cells. In the yeast *Saccharomyces*

* Corresponding author. Mailing address: Department of Biology, Indiana University, Jordan Hall A305, Bloomington, IN 47405. Phone: (812) 855-8883. Fax: (812) 855-6705. E-mail: donahue@bio.indiana.edu.

† Present address: Whitehead Institute for Biomedical Research Cambridge, MA 02142-1479.

cerevisiae a general mechanism for mRNA decay whereby mRNA is first deadenylated down to approximately 10 A residues, which triggers the decapping of mRNA and subsequent 5′-to-3′ degradation of the message, has been proposed (2, 40). The 5′-to-3′ exonuclease that appears responsible for the bulk of mRNA degradation is encoded by the *XRN1* gene.

In addition to degradation of mRNA, poly(A) tails have also been implicated to be involved in translation. For example, poly(A)-tailed mRNAs are translated more efficiently than their deadenylated counterparts in rabbit reticulocyte lysates (31). In addition, genetic studies of yeast have implicated a connection between the poly(A) tails and the poly(A) binding protein (PABP) with translation of mRNA. A mutation in the *SPB4* gene encoding one of the 60S ribosomal proteins can suppress the lethality resulting from a deletion of the *pab1* gene, which encodes the major PABP in budding yeast. This finding suggested that PABP might be involved in translation (50). PABP-poly(A) complex has also been shown to enhance translation efficiency in vitro by recruiting 40S subunits to mRNAs, and this enhancement was cap binding protein (eIF-4E) independent (56). Recent studies have established a functional relationship between the cap structure at the 5′ end of mRNA and the poly(A) tail of mRNA. The Pab1 protein can copurify and coimmunoprecipitate with the eIF-4γ subunit of the eIF-4F complex in yeast extracts (57), suggesting that the 3′ and 5′ ends of mRNA may be near each other when mRNA is actively translated. Thus, a complex interplay exists between the cap and the poly(A) tail in both mRNA stability and translation initiation (6, 56, 57).

In this study, we put the yeast *HIS4* gene under the transcriptional control of the pol I ribosomal DNA (rDNA) promoter/enhancer region (referred to as the *rhis4* gene) and extensively characterized the transcription of this gene, the 5′ and 3′ processing of transcripts, and the translational expression of *rhis4* mRNA in yeast. Our analysis shows that RNA pol I promotion of *HIS4* results in two mRNA species; one is the same size as the *HIS4* mRNA, and the other is 1.3 kb longer than the *HIS4* mRNA and is bicistronic. Surprisingly, both mRNAs appear to be polyadenylated despite transcription by RNA pol I. An *xrn1*Δ strain or a genetically isolated suppressor of *rhis4*, *rhis1* (*rhs* stands for *rhis4* suppressor) which encodes a defective *xrn1* gene, results in a 9- to 10-fold increase in the combined levels of *rhis4* mRNAs. This observation suggests that the majority of the *rhis4* mRNAs are transcribed by pol I and degraded rapidly due to the absence of a cap structure. Despite a large increase in the level of *rhis4* mRNAs in an *rhs1* (*xrn1*) mutant strain, the level of His4 protein remains low relative to a *HIS4*$^+$ strain. Our data suggest that in yeast cells, polyadenylation of *rhis4* mRNAs is able to occur independently of RNA pol II transcription. In addition, our results point to the cap as being an essential element for efficient translation initiation in yeast cells.

MATERIALS AND METHODS

Yeast strains and genetic methods. Strains used in this work are listed in Table 1. Standard genetic methods and media have been previously described (52).

For construction of the *rhis4* allele, a 2.5-kb *Eco*RI restriction fragment containing the enhancer/promoter region from plasmid pJ10-2 (14), which contains a unit repeat of the rDNA cistron, was introduced at a unique *Eco*RI restriction site at positions −51 to −50 (A of translational initiation codon; AUG is the +1 position) in the *HIS4* leader region of the Ura3$^+$ integrating plasmid p−51/−50 (7). Plasmid p1179 has the *Eco*RI rDNA fragment in the orientation that would allow pol I rDNA transcription to initiate toward the *HIS4* coding region as determined by restriction analysis. This plasmid was used to transform yeast strain TD28 to Ura$^+$. This plasmid when integrated into the *HIS4* locus results in a leaky His$^+$ phenotype as a result of an upstream and out-of-frame AUG codon now present in the *HIS4* leader region (see Results). Transformants with a leaky His$^+$ phenotype were purified by streaking and plated on 5′-fluoro-orotic acid plates to enrich for loss of the vector sequences (4). Ura3$^-$ strains having a leaky His$^+$ phenotype represented cells containing the *rhis4* allele.

TABLE 1. Strains used

Strain	Genotype
45-3B	*MAT*α *ura3-52 leu2-3,112 his4*Δ*-401*
1566-18B	*MAT*α *his4-316 ura3-52 ino1-13*
1567-5A	*MAT***a** *his4-316 ura3-52 trp1*
1567-32C	*MAT*α *his4-316 ura3-52 leu2-3,112 ade5 inol-13*
HH828	*MAT*α *rhis4 ura3-52 leu2-3,112 XRN1::URA3*
HH879	*MAT***a** *ura3-52 ino1-13* p1254 (YEp24-*URA3-HIS4*)
HH880	*MAT***a** *ura3-52 ino1-13 upf1*Δ*::URA3*
HH881	*MAT***a** *ura3-52 ino1-13 rhis4 upf1*Δ*::URA3*
HH882	*MAT***a** *ura3-52 ino1-13 rhis4-AGG upf1*Δ*::URA3*
HJ35	*MAT***a** *ura3-52 ino1-13 rhis4 rhs1* (*xrn1*)
HJ224	*MAT*α *rpa135::LEU2 ade2-1 ura3-1 his3-11 trp1-1 leu2-3,112 can1-100* pNOY102 (plasmid carrying *GAL7*-35S rDNA [44])
HJ239	*MAT***a** *ura3-52 ino1-13 rhis4-AGG*
HJ291	*MAT***a** *ura3-52 ino1-13 rhis4-AGG*
HJ307	*MAT***a** *ura3-52 rhis4-AGG gal2*
HJ320	*MAT*α *ura3-52 leu2-3,112 rhis4 gal2*
HJ322	*MAT***a** *ura3-52 leu2-3,112 trp1-1 rhis4*
HJ325	*MAT***a** *ura3-52 leu2-3,112 rhis4*
HJ332	*MAT*α *ura3-52 inol-13*
HJ336	*MAT***a** *ura3-52 leu2-3,112 HIS4*
HJ337	*MAT***a** *ura3-52 leu2-3,112 rhis4*
HJ339	*MAT*α *ura3-52 leu2-3,112 rhis4-AGG*
HJ343	*MAT*α *ura3-52 leu2-3,112 trp1-1 HIS4 rpa135*Δ*::LEU2* pNOY102
HJ346	*MAT***a** *ura3-52 leu2-3,112 HIS4 rpa135*Δ*::LEU2* pNOY102
HJ350	*MAT***a** *ura3-52 leu2-3,112 trp1-1 rhis4 rpa135*Δ*::LEU2* pNOY102
HJ351	*MAT***a** *rhis4 ura3-52 trp1 rpa135*Δ pNOY102
HJ354	*MAT***a** *leu2-3,112 ino1-13 trp1 rhis4-AGG rpa135*Δ pNOY102
HJ355	*MAT*α *ura3-52 leu2-3,112 rhis4 rpa135*Δ*::LEU2* pNOY102
HJ363	*MAT***a** *rhis4 ura3-52 rhs1* (*xrn1*)
HJ364	*MAT*α *ura3-52 trp1-1 rhis4 rhs1* (*xrn1*)
HJ399	*MAT***a** *leu2-3,112 ino1-13 rhis4-AGG*
HJ442	*MAT***a** *ura3-52 leu2-3,112 rhis4 rpa135*Δ*::LEU2 rhs1* (*xrn1*) pNOY102
HJ429	*MAT*α *rhis4 leu2-3,112 ura3-52*
HJ549	*MAT***a** *ura3-52 ino1-13 leu2-3,112 rhis4 xrn1*Δ*::URA3*
HJ556	*MAT***a** *ura3-52 ino1-13 rhis4 xrn1*Δ*::URA3*
HJ569	*MAT***a** *ura3-52 ino1-13 leu2-3,112 rhis4-AGG xrn1*Δ*::URA3*
TD28	*MAT***a** *ura3-52 ino1-13*
TD237	*MAT***a** *ura3-52 ino1-13 rhis4*

For construction of the *rhis4-AGG* allele, a 2.2-kb *Pvu*II-*Nhe*I DNA fragment from plasmid p1179 ligated into the phage vector Mp18. The oligonucleotide 5′-AACTGCTTTCGCCTGAAGTACCTCC-3′, containing an A-to-C base change (underlined), was used to perform site-directed mutagenesis. This base change results in the AUG codon, beginning at the +1 position of the pol I-promoted transcript, being changed to AGG. A 1.3-kb *Sph*I DNA fragment containing the mutation was isolated and substituted for the wild-type *Sph*I fragment of plasmid pJ10-2, which contains a unit repeat of rDNA (14), to yield plasmid p1679. The 2.5-kb *Eco*RI restriction fragment containing the rDNA enhancer/promoter region from plasmid p1679 was subcloned into an *Eco*RI restriction site of p−51/−50 (7), to yield plasmid p1696. This plasmid was used to construct a yeast strain containing the *rhis4-AGG* allele on chromosome III, identically to that described above for the construction of an *rhis4* strain.

Isogenic *HIS4* (TD28), *rhis4* (TD237), and *rhis4-AGG* (HJ291) strains containing an *xrn1*Δ mutation were constructed by transformation using a *Sal*I DNA fragment derived from plasmid p*dst2-1* (13), which contains a *dst2* (*xrn1*)*::URA3* deletion/disruption mutation. Deletion or disruption of the *XRN1* gene in these strains was confirmed by Southern blot analysis. The *rhs1* (*xrn1*) suppressor mutant was identified as a strong His$^+$ revertant of yeast strain TD237. Genetic analysis identified a suppressor mutant unlinked to the *rhis4* locus that conferred

a slow-growth phenotype. The *RHS1* (*XRN1*) gene was cloned by transformation from a pCT3 wild-type genomic library (kindly provided by Craig Thompson) by complementation of the slow-growth phenotype. Restriction analysis of complementing plasmids showed the DNA insert to have the same restriction pattern as the *XRN1* gene. The *URA3* gene was integrated adjacent to the *XRN1* locus of the *rhis4* strain HJ429 to generate yeast strain HH828. Yeast strain HH828 was then crossed to the *rhs1* yeast strain HJ35, and diploids were subjected to tetrad analysis. For each of the 15 four-spore tetrads analyzed, the two meiotic products with the *rhs1* slow-growth phenotype were Ura^-, whereas the other two meiotic products with a wild-type growth phenotype were Ura^+, indicating *rhs1* to be very tightly linked to *XRN1*. Finally, an *rhs1* mutant does not complement the slow-growth phenotype associated with an *xrn1* deletion/disruption strain. These studies taken together indicate that the *rhs1* locus is a mutant allele of the *XRN1* gene.

Isogenic *HIS4* (TD28), *rhis4* (TD237), and *rhis4-AGG* (HJ291) strains containing a *upf1*Δ mutation were constructed by transformation using an *Eco*RI-*Bam*HI DNA fragment derived from plasmid pLB65 (kindly provided by Michael Culbertson), which contains a *upf1::URA3* deletion/disruption mutation. Deletion/disruption of the *UPF1* gene in these strains was confirmed by Southern blot analysis.

Relevant strains containing an *rpa135*Δ mutation were constructed in a two-step process. First, yeast strains TD28 (*HIS4*$^+$), HJ320 (*rhis4*), HJ307 (*rhis4-AGG*), and HJ35 (*rhis4 rhs1*) were crossed to strains 1567-32C, 1567-5A, 1566-18B, and HJ322, respectively, to generate ascospores HJ336 (*HIS4*$^+$), HJ325 (*rhis4*), HJ339 (*rhis4-AGG*), and HJ363 (*rhis4 rhs1*) that grow well on YEPGal medium. In the second step, HJ336 was crossed to yeast strain NOY408-1D. The other three strains were crossed to either HJ343 or HJ350, ascospore derivatives of NOY408-1A or NOY408-1D, both of which contain an *rpa135::LEU2* mutation and transcribe rDNA from a *GAL7* pol II promoter construct on a plasmid (44). Ascospores used for our analysis are HJ346 (*HIS4*$^+$), which has a His^+ phenotype on galactose-containing medium and shows no growth on YEPD medium; HJ350 (*rhis4*), which is His^- on galactose-containing medium and shows no growth on YEPD medium; HJ354 (*rhis4-AGG*), which is His^- on galactose-containing medium and shows no growth on YEPD medium; and HJ442 (*rhis4 rhs1*), which is His^- on galactose-containing medium and shows no growth on YEPD medium. The His^- phenotype observed in these latter three strains is a result of the *rpa135*Δ mutation abrogating the leaky His^+ phenotype normally associated with *rhis4* and *rhis4-AGG* strains as a result of these alleles no longer being transcribed by RNA pol I.

To test whether the first 50 nt of leader sequence derived from *rhis4-AGG* have any inhibitory effect on translation, two DNA oligonucleotides containing the complementary sequences of this 50-nt region were hybridized and subcloned into the *Eco*RI site located at positions −51 to −50 of a *HIS4-lacZ* fusion construct (7). Yeast total protein was isolated and β-galactosidase specific activity was assayed as previously described (10).

RNA methods. The 5′ end of the *rhis4* transcripts was mapped by primer extension as previously described (7). Northern blot analysis was performed as previously described (7), with minor modifications. Twenty micrograms of total RNA was resolved on a 1% agarose gel under denaturing conditions (6% formaldehyde) and then transferred to a nitrocellulose membrane (51). The membrane was incubated with 20 ml of prehybridization buffer containing 50% deionized formamide, 5× SSC (1× SSC is 0.15 M NaCl plus 0.015 M sodium citrate), 10× Denhardt's reagent, and 2 mg of denatured calf thymus DNA. Radioactive probes were generated by using a random prime kit (Boehringer Mannheim) according to the manufacturer's protocol, using [α-^{32}P]ATP (3,000 Ci/mmol; Amersham). *HIS4* mRNA levels were quantitated with a PhosphorImager (Molecular Dynamics) using *ACT1* mRNA (actin) levels as an internal control.

The sites of polyadenylation of *HIS4* and *rhis4* mRNAs were determined by reverse transcription-PCR (RT-PCR) by the method of Frohman (17) and with some modification by using the Perkin-Elmer Cetus GeneAmp RNA PCR kit. In the first step, 100 ng of poly(A)$^+$ RNA from a *HIS4* or *rhis4* strain was mixed with oligonucleotide QT [5′-Qo-QI-d(TTTTTTTTTTTTTTTT)-3′], to generate a cDNA pool by reverse transcriptase. In the first PCR, oligonucleotides Qo [5′-d(CCAGTGAGCAGAGTGACG)-3′] and HIS2057 [5′-d(CGGTGACTAT TCAAGTGG)-3′], corresponding to positions +2157 to +2174 in the *HIS4* coding region, were used to amplify *rhis4s*, *rhis4l*, and *HIS4* mRNAs. In the second-round PCR, oligonucleotides QI [5′-d(GAGGACTCGAGCTCAAGC)-3′] and HIS2199 [5′-d(GGTTACGCTAGGCAGTAC)-3′], corresponding to positions +2200 to +2217 in the *HIS4* coding region, were used to amplify *rhis4s* and *HIS4* mRNAs, and oligonucleotides QI and HIS3056 [5′-d(CGAGAA GAGATACACACC)-3′] were used to amplify *rhis4l* mRNA. Oligonucleotide HIS3056 corresponds to positions +318 to +335 in the *YCL184* coding region. The PCR fragments from *rhis4s* and *HIS4* mRNAs were digested with *Sac*I within QI and *Xba*I corresponding to position +2328 in the *HIS4* coding region, subcloned into the *Sac*I and *Xba*I restriction sites in M13, and analyzed by DNA sequencing. The PCR fragment from *rhis4l* mRNA was digested with *Sac*I within QI and *Sph*I corresponding to position +421 in the *YCL184* coding region, subcloned into the *Sac*I and *Sph*I sites of M13, and analyzed by DNA sequencing.

Nuclear run-on experiments were performed as described by Elion and Warner (14). Yeast cells were permeabilized and labeled with [α-^{32}P]UTP for 15 min in the absence or presence of 10 or 100 μg of α-amanitin per ml. Total ^{32}P-labeled RNA was then extracted from the cells and used as a probe for Southern hybridization. Immobilized DNA fragments derived from plasmids containing the coding regions of the *HIS4* gene, the *URA3* gene, and the yeast transposable element Ty served as a controls for pol II transcription. A plasmid containing the 28S transcribed region of rDNA served as a control for pol I transcription. The *HIS4* plasmid (B115) was restricted with *Eco*RI, the Ty plasmid (B80) was restricted with *Bgl*II, and the plasmid (p1241) containing the 28S rDNA was restricted with *Eco*RI. The results of these experiments were quantitated with a PhosphorImager. For each experiment shown in Fig. 4A, the amount of radioactivity detected hybridizing with Ty, *HIS4*, or *rhis4* DNA was normalized to the amount of radioactivity hybridizing to rDNA. Each of these values are expressed in Fig. 4B as a percentage of the respective mRNA/rRNA species ratio determined in the absence of α-amanitin treatment.

Immunoprecipitations with polyclonal anti-m^{7}G antibodies (42) (kindly provided by R. Parker and E. Lund) were performed as described by Muhlrad et al. (40). Prior to immunoprecipitation, total RNA isolated from a *HIS4* or *rhis4 rhs1* (*xrn1*) strain was hybridized to an oligonucleotide, 5′-d(GGAGAACTG GAGAATCTCTTC)-3′, that is complementary to positions +90 to +111 in the *HIS4* coding region. RNA-DNA duplex was cleaved with RNase H, resulting in 157- and 197-nt fragment for *HIS4* and *rhis4* mRNAs, respectively. The supernatant and pellets were subjected to electrophoresis on a 10% polyacrylamide gel with 6 M urea. The cleavage products of *rhis4* and *HIS4* mRNAs were detected by Northern blot analysis using a ^{32}P-labeled antisense RNA complementary to positions −50 to +97 in the *HIS4* gene. The membrane was exposed in a PhosphorImager screen (Molecular Dynamics) for 3 days and visualized in a PhosphorImager (Molecular Dynamics). The cleaved and intact *HIS4* and *rhis4* were detected and recorded. As a control for immunoprecipitation, the same membrane was hybridized with a ^{32}P-labeled DNA probe complementary to the *MFA2* gene, and the intact *MFA2* mRNA was visualized in a PhosphorImager after 1 day of exposure.

Western blot analysis. Protein extracts were prepared from yeast and analyzed by Western blots as previously described (11, 29). Rabbit polyclonal antisera directed against either the His4 protein (1:10,000) or the eIF-2γ (1:25,000) were used as the primary probes in an overnight incubation. Peroxidase-conjugated anti-rabbit immunoglobulin G (Sigma) was used as the secondary probe (1:25,000) in a 2-h incubation. The antibody-antigen complex was detected by the Amersham ECL system according to the manufacturer's protocol. To quantitate the protein levels, the film was scanned by a densitometer (Molecular Dynamics). For each lane, the density of the His4 band was compared to the density of the eIF-2γ protein band, as an internal control.

RESULTS

Construction of *rhis4* strains. The main aim of this study was to elucidate the possible functions of the cap structure of mRNA in yeast by generating and characterizing an uncapped cellular mRNA in vivo. The *rhis4* gene was constructed (Fig. 1; also see Fig. 3) such that the *HIS4* gene could be transcribed by a pol I-specific promoter. The construct consists of the 2.5-kb *Eco*RI restriction fragment containing the rDNA enhancer/promoter region (14) that was introduced upstream at a unique *Eco*RI restriction site at positions −51 to −50 (A of translational initiation codon; AUG is the +1 position) in the *HIS4* leader (7). This promoter fusion construct was then introduced at the *HIS4* locus by the integration-excision method. Transcription from this construct is predicted to start at the 35S rDNA gene transcription initiation site, resulting in the *rhis4* mRNA having a 5′ untranslated region (UTR) 100 nt in length. The first 50 nt of the leader region of the *rhis4* mRNA will be derived from the 35S rRNA, and the downstream 50 nt of the 5′ UTR of *rhis4* mRNA are predicted to be derived from the *HIS4* mRNA leader.

Characterization of the *rhis4* mRNAs. To characterize *rhis4* expression, we first measured the steady-state level of the *rhis4* transcript by Northern blot analysis using a ^{32}P-labeled probe which contains sequences complementary to the downstream coding region of the *HIS4* gene. As shown in panel 2 of Fig. 1B, two different-size *rhis4* mRNAs are detected (middle lane); one transcript, *rhis4s*, is approximate the same size as the wild-type *HIS4* mRNA, while the other transcript, *rhis4l*, is approximately 1.3 kb longer than the *HIS4* and *rhis4s* mRNAs. The combined steady-state level of the *rhis4s* and *rhis4l* mRNAs was quantitated to be in the range of 50 to 100% of

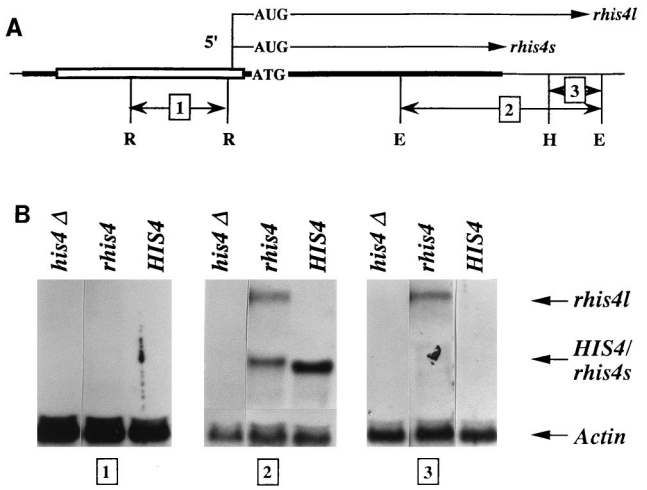

FIG. 1. Northern blot analysis of the *rhis4s* and *rhisl* mRNAs. (A) Schematic representation of the *rhis4* gene. The open bar represents the rDNA enhancer/promoter region, and the solid bar represents *HIS4* sequences. (B) Twenty micrograms of total RNA was isolated from yeast strains 45-3B (*his4*Δ), TD237 (*rhis4*), and TD28 (*HIS4*$^+$) and analyzed by Northern blotting using ^{32}P-labeled probes complementary to different regions of the *rhis4* construct. Location of the probes are shown in panel A. Probe 1 is a 1.5-kb *Rsa*I DNA fragment derived from plasmid pJ10-2 (14) and is complementary to the region upstream of the predicted 35S transcription initiation site. Probe 2 is a 2.7-kb *Eco*RI DNA fragment from plasmid B115 (12) and is complementary to the *HIS4* distal coding region, the 3′ UTR of the *HIS4* gene, and the 5′ region of the *YCL184* gene. The *YCL184* gene is located downstream of the *HIS4* gene and is predicted to be transcribed in the same direction as the *HIS4* gene (48). Probe 3 is an approximately 0.5-kb *Hin*dIII-*Eco*RI fragment derived from plasmid B115 which is located downstream of the *HIS4* 3′ UTR. All filters were coprobed with a 3.0-kb *Eco*RI-*Bam*HI DNA fragment containing the entire actin gene. R, *Rsa*I; E, *Eco*RI; H, *Hin*dIII.

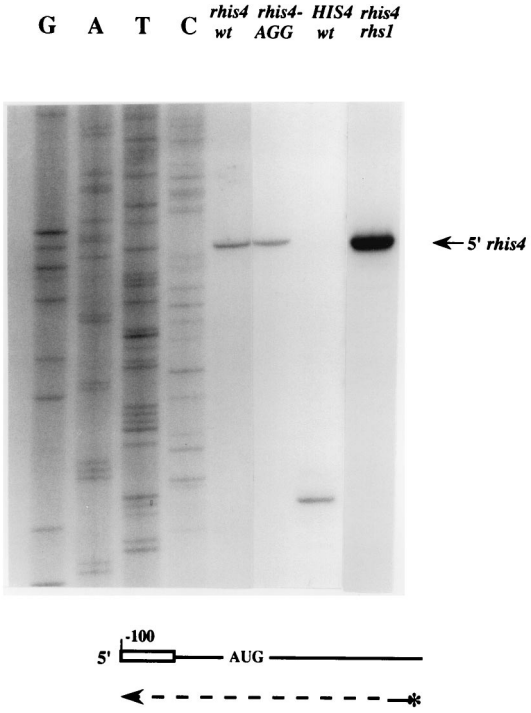

FIG. 2. Primer extension analysis of the *rhis4* and *rhis4-AGG* mRNAs. A 50-μg sample of total RNA isolated from yeast strains TD28 (*HIS4*$^+$), TD237 (*rhis4*), HJ291 (*rhis4-AGG*), and HJ35 (*rhis4 rhs1* [*xrn1*]) was characterized by primer extension analysis. Five picomoles of the ^{32}P-labeled oligonucleotide 38, 5′d(CATCAATTAACGGTAGAATCGG)3′, which is complementary to positions +10 to +31 in the *HIS4* coding region, was used as a primer. The transcription initiation site of the *rhis4* and *rhis4-AGG* mRNAs is indicated by an arrow. A DNA sequencing ladder, GATC, from *rhis4* DNA, is presented. *wt*, wild type.

the *HIS4* mRNA level, using actin mRNA levels as an internal control.

To map the 5′ and 3′ boundaries of the *rhis4s* and *rhis4l* mRNAs, we used ^{32}P-labeled probes from different regions of the *rhis4* gene. Probe 1 (Fig. 1A) was a 1.5-kb *Rsa*I fragment complementary to the region upstream of the 35S rDNA transcription initiation site. Probe 3 (Fig. 1A) was derived from the region downstream of the *HIS4* locus and excludes sequences that are complementary to the 3′ UTR of *HIS4*. As shown in panel 1 of Fig. 1B, neither the *rhis4s* nor the *rhis4l* mRNA is detected with probe 1, suggesting that the transcription initiation site of both species of *rhis4* mRNA is located downstream of probe 1. Probe 3 does not detect the *HIS4* mRNA as expected, nor does it detect the *rhis4s* mRNA. Thus, *rhis4s* mRNA appears to have 5′ and 3′ boundaries similar to those of the *HIS4* mRNA. In contrast, probe 3 detects the *rhis4l* mRNA. Thus, *rhis4l* mRNA appears to have a 5′ boundary similar to that of *rhis4s* mRNA, but *rhis4l* is longer at the 3′ end than the *rhis4s* and *HIS4* mRNAs.

To determine whether the two species of *rhis4* mRNAs have the same transcription initiation site, the 5′ ends of the *rhis4* transcripts and the *HIS4* mRNA were analyzed by primer extension analysis using an oligonucleotide complementary to positions +10 to +31 in the *HIS4* coding region. Figure 2 shows that the transcription initiation site of the *HIS4* gene maps to position −60 relative to the translation initiation codon, as previously described (second lane from right) (12, 43). In contrast, the transcription start site of the *rhis4* gene is located at position −100 (Fig. 2, fourth lane from right, indicated by an arrow), which corresponds to the predicted 35S rDNA transcription initiation site (1, 33). No primer extension product was detected either upstream or downstream of the pol I transcription start site. This analysis in combination with the Northern analysis indicates that both species of *rhis4* mRNAs are initiated at the pol I transcription initiation site.

To map the 3′ ends of both *rhis4* mRNAs, RT-PCRs were performed and the products were subcloned to an M13 vector for DNA sequencing. In total, four clones from the *HIS4* PCR pool, four clones from the *rhis4s* PCR pool, and five clones from the *rhis4l* PCR pool were sequenced. Figure 3A summarizes the results, and Fig. 3B shows one of the sequences from each of the mRNA PCR pools. Three different polyadenylation sites were identified among the four clones from the *HIS4* pool. Two clones mapped the polyadenylation site to be 137 nt downstream of the *HIS4* translational stop codon (Fig. 3A, underlined T next to top arrowhead), and the other two clones mapped polyadenylation sites to be either 80 or 84 nt downstream of the *HIS4* translational stop codon, respectively (Fig. 3A, two G's flanking leftmost arrow). All four clones from the *rhis4s* pool mapped the polyadenylation site to be 137 nt downstream of the translational stop codon at *HIS4*, identical to what was observed for two of the *HIS4* clones. Four clones from the *rhis4l* pool mapped the polyadenylation site to be 102 nt downstream of the translational stop codon of the *YCL184* gene (Fig. 3A, underlined C next to bottom arrowhead), and the remaining clone from the *rhis4l* pool mapped a site to be 119 nt downstream of the *YCL184* stop codon (Fig. 3A, underlined C to the right). As for other yeast genes, polyadenylation starts right before or after an adenosine residue (24). In addition, there is more than one polyadenylation site for *HIS4*

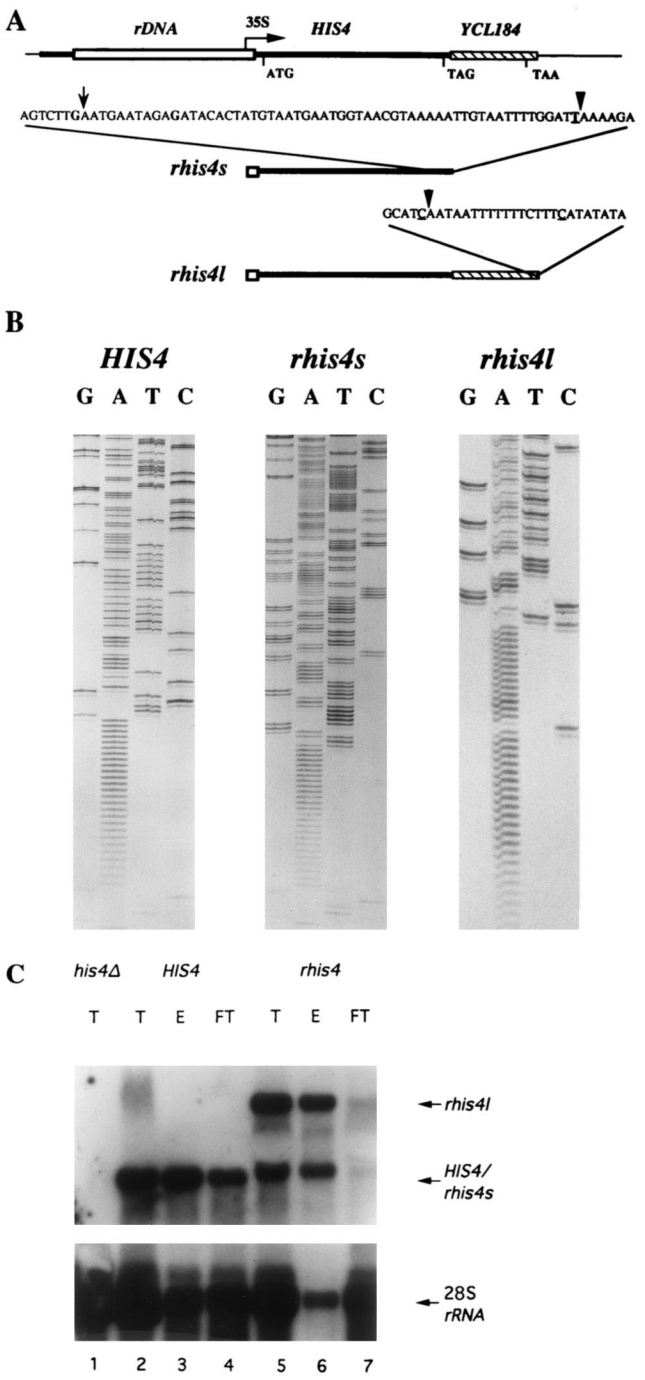

FIG. 3. RT-PCR mapping of the site of polyadenylation of *rhis4* mRNA species and analysis of their ability to bind oligo(dT) cellulose. (A) Schematic summary of RT-PCR mapping of the *rhis4s* and *rhis4l* mRNA polyadenylation sites relative to the 3′ UTR of the *HIS4* and *YCL184* genes, respectively. The complete sequence of the 3′ UTRs from the *HIS4* and *YCL184* genes relative to their respective translation stop codons is not shown. The relevant nucleotides corresponding to the sites of polyadenylation in different RT-PCR clones is described in the text. (B) Example of the DNA sequence of one RT-PCR clone obtained for each mRNA. The corresponding sites of polyadenylation are indicated by an arrow or arrowhead (left to right) in panel A. (C) Total RNA isolated from different yeast strains was passed over an oligo(dT) column. Total RNA (T; 20 μg), flowthrough fractions (FT; 20 μg), and RNA which bound and was eluted from the column (E; 5 μg) were then subjected to Northern blot analysis using a ^{32}P-labeled *HIS4* probe (top panel). Filters were washed and then reprobed with a ^{32}P-labeled probe from 28S rDNA (bottom panel). Lanes: 1, total RNA from the *his4*Δ strain, 45-3B; 2 to 4, total, eluted, and flowthrough fractions from the *HIS4*$^{+}$ strain, TD28; 5 to 7, total, eluted and flowthrough fractions from the *rhis4* strain, TD237.

or *rhis4l* as observed for other yeast genes. The *YCL184* gene was identified as part of the chromosome III sequencing project and represents the first gene downstream of *HIS4* that is predicted to be transcribed in the same direction (48). Interestingly, the *rhis4l* mRNA appears to be a bicistronic mRNA.

To determine whether the majority of *rhis4* mRNAs are polyadenylated, poly(A)$^{+}$ RNA was separated from poly(A)$^{-}$ RNAs by oligo(dT)-cellulose chromatography. Total RNA, RNAs bound to the oligo(dT) column (eluted from column), and RNAs that did not bind to the oligo(dT) column (flowthrough) were analyzed by Northern blotting using a probe complementary to the coding region of the *HIS4* gene. Blots were then reprobed with a ^{32}P-labeled probe from the 28S transcribed region of rDNA (Fig. 3C, bottom panel) to determine the efficiency of separation of poly(A)$^{+}$ RNA from poly(A)$^{-}$ RNA. As shown in Fig. 3C, the amount of *HIS4* mRNA that bound to oligo(dT) was more than that detected in the flowthrough fraction (lanes 4 and 5). *rhis4* mRNAs also bound to the oligo(dT) column (lanes 6 and 7), suggesting that the majority of *rhis4s* and *rhis4l* mRNAs are polyadenylated.

***rhis4* is transcribed by pol I.** One way to distinguish pol I and pol II transcription is to determine whether transcription is sensitive to the specific pol II inhibitor α-amanitin. Detergent-permeabilized yeast cells were used to determine the effects of α-amanitin on *rhis4* transcription. As shown by Elion and Warner (14), permeabilized cells provide a convenient means to examine run-on transcription in vivo. Permeabilized cells were labeled with [α-^{32}P]UTP for 15 min in the absence or presence of 10 or 100 μg of α-amanitin per ml. Total ^{32}P-labeled RNA was then extracted from these cells and used as a probe for Southern hybridization. Immobilized DNA fragments were derived from plasmids containing the coding region of the *HIS4* gene, the *URA3* gene, the yeast transposable Ty element, and the 28S transcribed region of rDNA. These plasmids allowed us to detect *rhis4* transcripts as well as detect other pol II and pol I transcripts which served as controls. The *HIS4* plasmid was restricted with *Eco*RI, which yields a fragment expected to hybridize with the ^{32}P-labeled *HIS4* or *rhis4* mRNA as well as a larger, vector fragment that contains the intact *URA3* gene. The Ty plasmid was restricted with *Bgl*II. Several *Bgl*II sites are contained in the DNA of the Ty element and should hybridize to the Ty transcript. The plasmid containing the 28S rDNA was restricted with *Eco*RI, which generates one fragment that will hybridize with rRNA.

As shown in Fig. 4A, cells labeled with [α-^{32}P]UTP in the presence of α-amanitin generate less *HIS4*, *URA3*, and Ty mRNAs than cells labeled with [α-^{32}P]UTP in the absence of α-amanitin. This result indicates that these genes are transcribed by pol II, as expected. In contrast, cells labeled with [α-^{32}P]UTP in the absence or presence of α-amanitin produce similar amounts of the *rhis4* mRNA and similar amounts of rRNA. Figure 4B shows the quantitation of these data whereby the amounts of the *HIS4*, *rhis4*, and Ty mRNAs are normalized to the level of hybridized rRNA. The relative levels of mRNAs isolated from the cells incubated in the absence of α-amanitin are expressed as 100%. Approximately 90% of *HIS4* and 85% of Ty transcription is inhibited by 100 μg of α-amanitin per ml. In contrast, *rhis4* transcription is not affected by α-amanitin. This results suggests that at least a significant portion of *rhis4* transcription is resistant to α-amanitin and therefore is under the control of the pol I promoter.

The *RPA135* gene, which encodes the second-largest subunit of pol I (60), is essential for the transcription of rDNA. A deletion of the *RPA135* gene causes cell death. However, an *RPA135* deletion strain can be rescued by having an rDNA

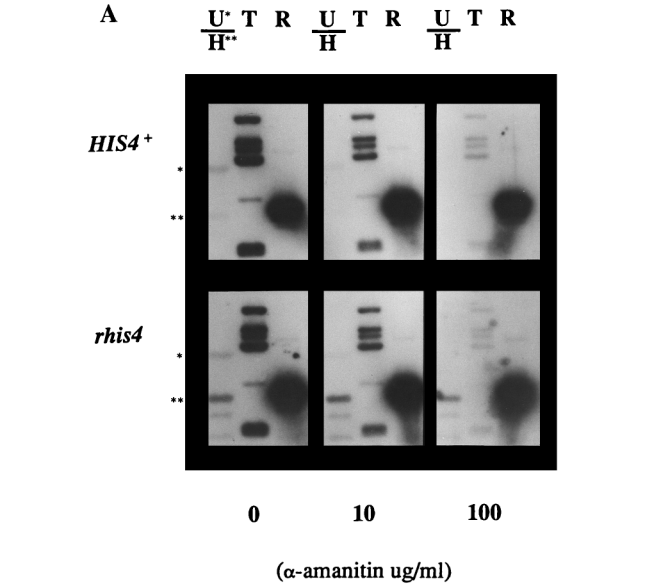

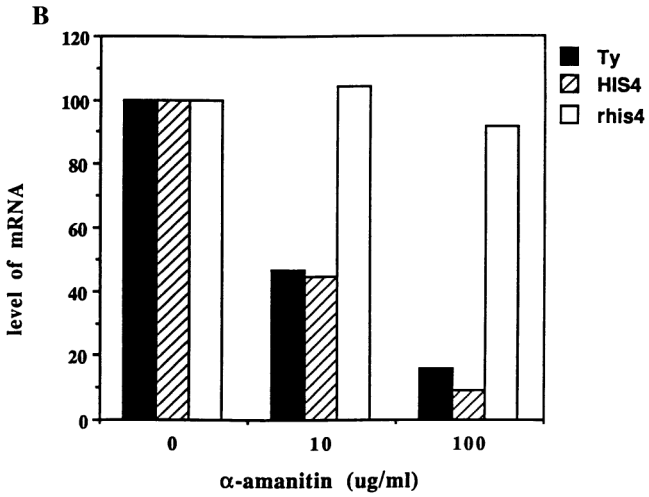

FIG. 4. Nuclear run-on experiments using permeabilized cells in the absence or presence of α-amanitin. (A) Permeabilized yeast strains TD28 (*HIS4*$^+$) and TD237 (*rhis4*) were incubated with [α-^{32}P]UTP in the absence or presence of 10 or 100 μg of α-amanitin per ml. Total RNA was extracted and used as a probe for Southern hybridization. DNA fragments immobilized on nitrocellulose correspond to *URA3* (top band of U/H), *HIS4* (bottom band of U/H), Ty elements (T), and 28S rRNA (R). (B) The quantitation of the data in panel A. The levels of Ty, *HIS4*, and *rhis4* mRNAs are normalized by the levels of hybridized rRNA. The relative level of mRNAs from cells incubated in the absence of α-amanitin is expressed as 100%.

cistron transcribed from a pol II promoter which is provided by a unit repeat of 35S rDNA fused to the *GAL7* promoter. Thus, the *rpa135*Δ strain can grow in medium containing galactose, which activates the *GAL7* promoter to transcribe rDNA (44). We used an *rpa135*Δ *rhis4 GAL7*-rDNA strain to obtain evidence whether pol I is responsible for the transcription of the majority of *rhis4* mRNA. The rationale was that if some of *rhis4* mRNA is transcribed by pol II, this amount of *rhis4* mRNA should not be altered by the *rpa135*Δ mutation. In contrast, if transcription of *rhis4* is under the control of pol I, *rhis4* mRNA should be absent in an *rpa135*Δ strain. Total RNA was isolated from strains containing the *rpa135*Δ mutation or the wild-type *RPA135* gene and was analyzed by Northern blot

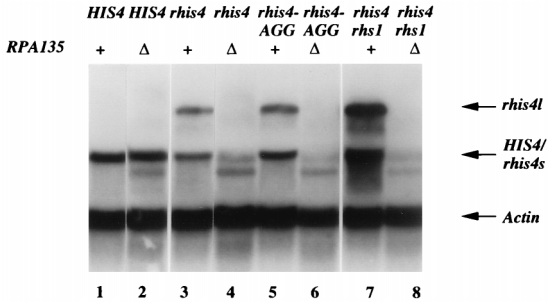

FIG. 5. Northern blot analysis of *rhis4* transcripts in an *rpa135*Δ genetic background. *RPA135*$^+$ and *rpa135*Δ strains were cultured in YEPG (galactose) medium, and then total RNA was isolated and analyzed by Northern blotting as described in Materials and Methods. Lanes: 1, *HIS4* (HJ332); 2, *HIS4 rpa135*Δ (HJ346); 3, *rhis4* (HJ322); 4, *rhis4 rpa135*Δ (HJ350); 5, *rhis4-AGG* (HJ399); 6, *rhis4-AGG rpa135*Δ (HJ354); 7, *rhis4 rhs1* (HJ364); 8, *rhis4 rhs1 rpa135*Δ (HJ442). The band observed in the *rpa135*Δ strains that migrates faster than the *HIS4* and *rhis4s* mRNA is a result of nonspecific cross-hybridization between an unknown RNA species derived from plasmid pNOY102 and the actin probe.

analysis. Figure 5 shows that *HIS4* transcription is not affected by a deletion of the *RPA135* gene (lanes 1 and 2). In contrast, there is no *rhis4l* mRNA detected in the *rpa135*Δ strain (lanes 3 and 4), indicating that *rhis4l* is promoted by pol I. There is a significant reduction of *rhis4s* mRNA detected in the *rpa135*Δ strain (lanes 3 and 4), suggesting that at least the majority of *rhis4s* transcription is promoted by pol I. The remaining *rhis4s* transcript is most likely a result of transcription from an overlapping pol II promoter in the rDNA pol I promoter region as previously reported (9).

The rate of *rhis4* transcription is higher than that of *HIS4*. Pol I transcription of *rhis4* is expected to generate uncapped mRNA. Thus, *rhis4* mRNA should represent the decapped intermediate form of mRNA in the yeast mRNA degradation process and should be degraded more quickly than pol II-promoted, capped *HIS4* mRNA. Nevertheless, the combined steady-state level of *rhis4s* and *rhis4l* is nearly comparable to that of *HIS4* mRNA. We therefore determined whether the steady-state level of *rhis4* mRNA is an underrepresentation of the rate of transcription at *rhis4* by comparing it to the rate of *HIS4* transcription (Fig. 6). Total ^{32}P-labeled RNAs were isolated from permeabilized cells after being labeled with [α-^{32}P]UTP for 1, 5, or 15 min. For these experiments, total RNA isolated from the *HIS4* strain or the *rhis4* strain was used

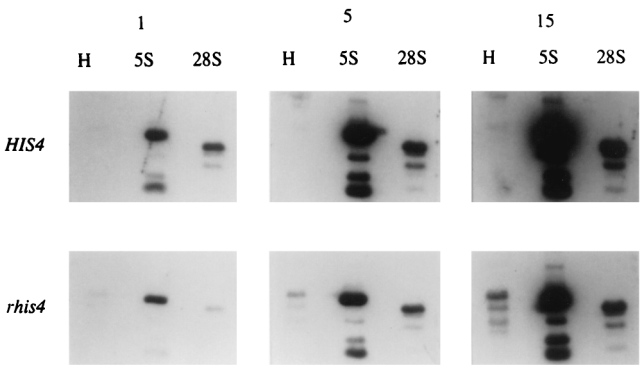

FIG. 6. Time course of *HIS4* and *rhis4* mRNA synthesis by nuclear run-on transcription assay. Yeast strains TD28 (*HIS4*) and TD237 (*rhis4*) were permeabilized, and aliquots of cells were labeled with [α-^{32}P]UTP for 1, 5, or 15 min. ^{32}P-labeled total RNA was isolated and used as probes for Southern hybridization to immobilized *HIS4* (H), 5S, and 28S DNA fragments.

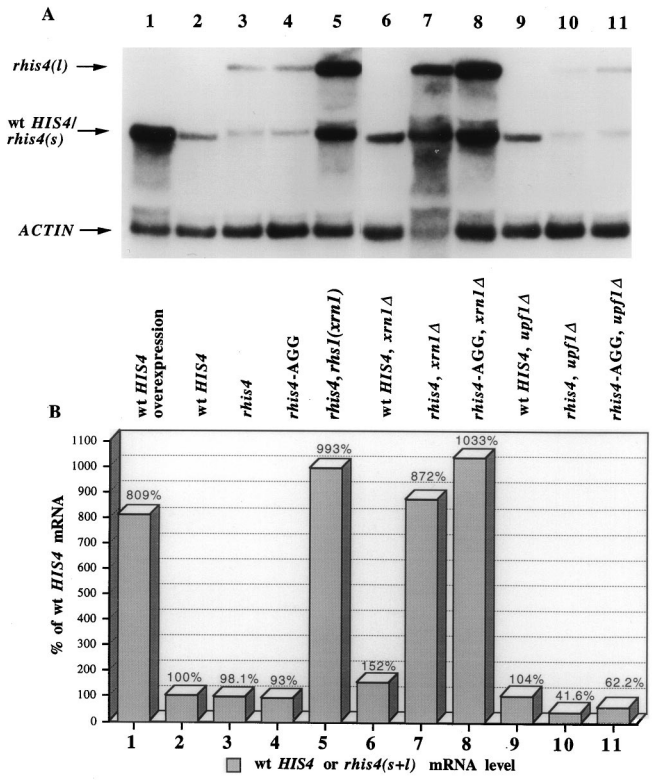

FIG. 7. Effects of mutations in *XRN1* and *UPF1* on *HIS4* and *rhis4* mRNA levels. (A) Total RNA was isolated from different yeast strains and subjected to Northern blot analysis as described in Materials and Methods. Total RNA was isolated from the following yeast strains: HH879 (which contains the *HIS4*$^+$ gene on a high-copy-number YEp24 vector; lane 1); TD28 (*HIS4*$^+$; lane 2); TD237 (*rhis4*; lane 3); HJ291 (*rhis4-AGG*; lane 4); HJ35 (*rhis4 rhs1* [*xrn1*], lane 5); HJ556 (*HIS4*$^+$ *xrn1*Δ; lane 6); HJ549 (*rhis4 xrn1*Δ; lane 7); HJ569 (*rhis4-AGG xrn1*Δ; lane 8); HH880 (*HIS4*$^+$ *upf1*Δ; lane 9); HH881 (*rhis4 upf1*Δ; lane 10); and HH882 (*rhis4-AGG upf1*Δ; lane 11). wt, wild type. (B) Bar graph illustrating the quantitation of *HIS4* or *rhis4* mRNA to actin mRNA levels for each lane in panel A as described in Materials and Methods. The ratio of *HIS4*$^+$ mRNA to actin mRNA in lane 2 represents the standard 100% level.

as a probe in Southern hybridization to immobilized DNA fragments corresponding to the coding region of the *HIS4* gene, the transcribed region of 5S rDNA (as a pol III transcription control), and the transcribed region of 28S rDNA (as a pol I transcription control). The restricted, immobilized DNA used for the *HIS4*/*rhis4* and 28S analysis is the same as described for Fig. 4. For the 5S analysis in Fig. 6, a plasmid containing the 2.5-kb *Eco*RI rDNA enhancer/promoter region was restricted with *Eco*RI and *Nde*I. The slower-migrating fragment (approximately 2.0 kb) contains the 5S gene free of other encoded rRNA sequences.

As shown in Fig. 6, the synthesis rates of both 5S rRNA and 28S rRNA appear quite high, probably as a result of multiple copies of these genes in the yeast genome. *HIS4* mRNA is barely detectable even after 15 min of labeling with [α-^{32}P]UTP. In contrast, *rhis4* mRNAs can be easily detected after 5 min of labeling with [α-^{32}P]UTP. This result suggests that the synthesis rate of the *rhis4* mRNA is higher than that of the *HIS4* mRNA despite the near equivalence of the steady-state levels. These data indicate that the lower level of the *rhis4* mRNA detected on Northern blots does not reflect the higher transcriptional level, presumably due to rapid decay of uncapped mRNAs.

Mutations in the *XRN1* gene increases the abundance of *rhis4* mRNAs. It has been reported that *XRN1* plays a critical role in mRNA decay after decapping (21, 27, 40). Thus, we reasoned that if the pol I-promoted *rhis4* mRNA is uncapped and rapidly degraded, *rhis4* mRNA would be predicted to accumulate in an *xrn1*Δ strain. Total RNA was isolated from strains containing either an *xrn1*Δ mutation or the wild-type *XRN1* gene and analyzed by Northern blots analysis. Figure 7 shows that the relative amount of the *HIS4* mRNA is approximately 50% higher in an *xrn1*Δ strain (lane 6) than in an *XRN1* strain (lane 2). In contrast, the combined levels of the *rhis4s* and *rhis4l* mRNAs are approximately ninefold higher in the *xrn1*Δ strain (8.4-fold for *rhis4s* mRNA and 9.6-fold for *rhis4l* mRNA) than in an *XRN1*$^+$ strain (compare lanes 3 and 7).

Several suppressor mutations that enhance the expression of the *rhis4* gene at the level of transcription have been isolated (28). As expected, *rhs1* corresponds to a mutation in the *XRN1* gene. Figure 2 shows that the transcription initiation sites of the *rhis4* mRNA in the parent strain and the *rhs1* strain are identical and correspond to the predicted pol I start site. In addition, an approximate 10-fold increase in the combined level of *rhis4* mRNAs (7.2-fold for *rhis4s* mRNA and 12.8-fold for *rhis4l* mRNA) is observed in the *rhs1* (*xrn1*) mutant genetic background (Fig. 7; compare lanes 3 and 5), consistent with that observed in the *xrn1*Δ strain. This increase in *rhis4* mRNA levels is also *RPA135* dependent (Fig. 5, lanes 7 and 8). The fact that a mutation in *xrn1* has such a specific and large effect on the level of *rhis4* mRNAs suggests that the pol I promotion of *rhis4* transcription leads to production of uncapped mRNA which is rapidly degraded. The effect of an *xrn1* mutation is then to reduce the cellular levels of 5′-to-3′ exonuclease activity that results in stabilization of the uncapped *rhis4* mRNAs.

***rhis4* mRNA that accumulates in an *xrn1* strain is not immunoprecipitated with anticap antiserum.** To directly determine if the *rhis4* mRNA that accumulates in the *rhs1* (*xrn1*) strain is uncapped, we immunoprecipitated the *rhis4* mRNA with antiserum directed against the cap structure (42). For these experiments, total RNA was isolated from cells, hybridized to an oligonucleotide that is complementary to the *HIS4* and *rhis4* mRNAs, and digested with RNase H. After immunoprecipitation, RNA was recovered from the pellets and supernatants and analyzed by Northern blot analysis using a ^{32}P-labeled probe that is complementary to positions −50 to +97 in the *HIS4* and *rhis4* mRNAs. This procedure was used as an attempt to maximize the efficiency of immunoprecipitation (41). As an internal control for immunoprecipitation, we also probed for the *MFA2* gene.

Prior to immunoprecipitation, we characterized the RNase H cleavage reaction and cleavage product, using two different oligonucleotides that hybridize to two different region of the *HIS4* coding region. Oligonucleotide 1 is complementary to nt +47 to +66 in the *HIS4* coding region, whereas oligonucleotide 2 is complementary to nt +90 to +111. As shown in Fig. 8A, oligonucleotide 1 generates a smaller RNase H cleavage product than oligonucleotide 2 when hybridized with total RNA from either a *HIS4*$^+$ or an *rhis4 xrn1*Δ strain. This is expected, as the former oligonucleotide is complementary to sequences that are located further upstream in the *HIS4* coding region. The RNase H cleavage products generated from the *rhis4 xrn1*Δ strain are also larger than the corresponding RNase H cleavage products which were generated from the *HIS4*$^+$ strain. This is consistent with the *rhis4* leader region being 40 nt longer than the *HIS4* leader (Fig. 2). The slower-migrating material observed in Fig. 8A presumably represents either the reciprocal *HIS4* or *rhis4* mRNA, RNase H cleavage

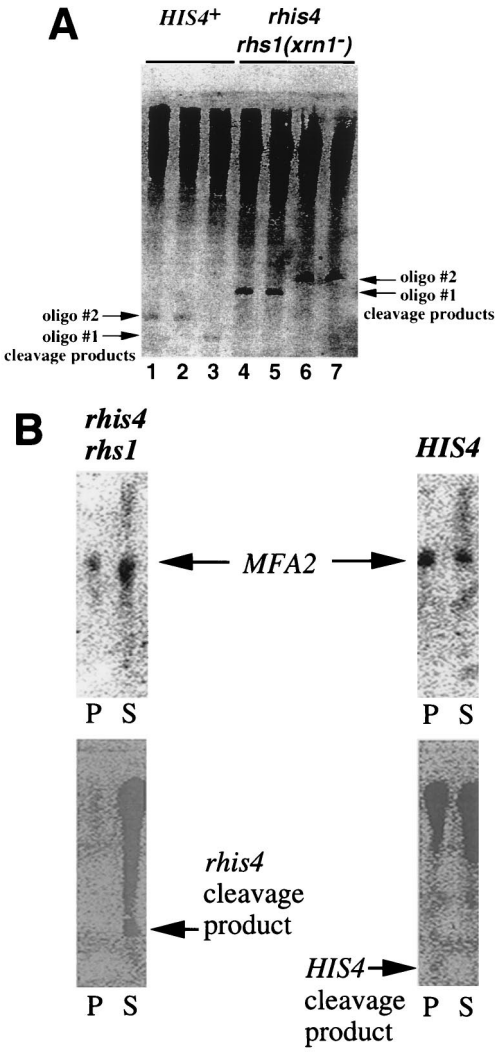

FIG. 8. (A) Total RNA from a *HIS4* strain and an *rhis4 rhs1* (*xrn1*) strain were hybridized with oligonucleotide (oligo) 1 or 2, complementary to the *HIS4* coding region from nt +47 to +66 or +90 to +111, respectively. RNA-DNA hybrids were treated with RNase H followed by electrophoresis in 6% acrylamide gels containing 8 M urea. Gels were then subjected to Northern blot analysis using an antisense RNA probe complementary to positions −50 to +97 in the *HIS4* gene. Lanes: 1 and 2, total RNA from a *HIS4*$^+$ strain hybridized with oligonucleotide 2 and cleaved with RNase H; 3, total RNA from a *HIS4*$^+$ strain hybridized with oligonucleotide 1 and cleaved with RNase H; 4 and 5, total RNA from an *rhis4 rhs1* (*xrn1*) strain hybridized with oligonucleotide 1 and cleaved with RNase H; 6 and 7, total RNA from an *rhis4 rhs1* (*xrn1*) strain hybridized with oligonucleotide 2 and cleaved with RNase H. (B) Immunoprecipitation of *HIS4* and *rhis4* mRNAs with anticap antiserum. Total RNA isolated from different strains was hybridized with oligonucleotide 2 (complementary to the *HIS4* coding region between positions +90 and +111), digested with RNase H, and immunoprecipitated with anticap antiserum as described in Materials and Methods. RNAs recovered from pellets (P) and supernatants (S) were analyzed by Northern blot analysis using two different probes, an antisense RNA complementary to positions −50 to +97 in the *HIS4* gene (bottom panels) and a random-primed probe complementary to the *MFA2* gene (top panels). The first two lanes represent precipitated and unprecipitated RNAs, respectively, from an *rhis4 rhs1* (*xrn1*) strain (HJ35). The last two lanes represent precipitated and unprecipitated RNAs from the *HIS4*$^+$ wild-type strain, TD28. The arrows in the bottom panels point to *rhis4* and *HIS4* mRNA RNase H cleavage products and correspond to the cleavage products characterized in panel A.

product, or full-length mRNA that did not hybridize with an oligonucleotide.

For the immunoprecipitation reactions presented in Fig. 8B, we used oligonucleotide 2. The *HIS4* cleavage product, which is presumably capped, could be detected in the immunoprecipitate and was not observed in the supernatant, albeit the detection resolution is quite low (Fig. 8B). In contrast, the *rhis4* cleavage product is not observed in the immunoprecipitate; rather, the *rhis4* cleavage product remained in the supernatant. As a control for these reactions, we found that the majority of the *MFA2* mRNA isolated from an *XRN1*$^+$ strain was immunoprecipitated with the anticap antiserum, whereas more *MFA2* mRNA from an *rhs1* (*xrn1*) strain remained in the supernatant, suggesting that *rhs1* (*xrn1*) stabilizes the decapped form of the *MFA2* mRNA, which does not immunoprecipitate. These results are consistent with the notion that the *rhis4* mRNA which accumulates in the *rhs1* (*xrn1*) strain is uncapped.

Construction of *rhis4-AGG* allele. The first three nucleotides from the pol I start position in rDNA are predicted to introduce an upstream and out-of-frame AUG codon at the immediate 5′ end of the *rhis4* mRNA (33). Thus, *rhis4* mRNA may be degraded by the nonsense-mediated decay pathway, and the *rhs1* or *xrn1*Δ mutation may stabilize the nonsense-mediated decay of *rhis4* mRNA (21). Therefore, we mutated the upstream and out-of-frame AUG to AGG by site-directed mutagenesis (for details, see Materials and Methods). The reason for choosing to mutate the AUG to AGG is that AGG has been identified as the first three nucleotides in precursor rRNA from *Drosophila* and *Xenopus* cells (15, 37). Therefore, we reasoned that an AUG-to-AGG change might not alter the start site for pol I transcription. The presence of this mutation was confirmed by DNA sequencing (data not shown), and the corresponding *rhis4* allele (*rhis4-AGG*) was inserted and replaced for the wild-type *HIS4* gene on chromosome III.

Figure 2 shows that the AGG mutation does not affect the transcription initiation site of *rhis4-AGG* mRNAs, as determined by primer extension analysis. *rhis4-AGG* also generates two mRNA species (Fig. 5, lane 5), *rhis4-AGGs* and *rhis4-AGGl*, with the same mobilities as the *rhis4s* and *rhis4l* mRNAs, respectively. In addition, the amounts of the *rhis4-AGG* transcripts are similar to those of the *rhis4* messages and are also sensitive to an *rpa135*Δ mutation (Fig. 5). The *xrn1*Δ mutation also results in a comparable increase in the combined level of the *rhis4-AGGs* and *rhis4-AGGl* transcripts (Fig. 7; compare lanes 4 and 8). Finally, to rule out nonsense-mediated decay as a mechanism for destabilizing *rhis4* mRNA, we measured the levels of *rhis4* and *rhis4-AGG* transcripts in a *upf1*Δ strain. Figure 7 shows that a *upf1*Δ mutation does not result in an increase in *rhis4s* or *rhis4-AGGs* mRNA or *rhis4l* and *rhis4-AGGl* transcripts, which are bicistronic (compare lanes 3 and 4 to lanes 10 and 11, respectively). These data suggest that a large majority of *rhis4* transcription products are unstable, not as a result of nonsense-mediated decay but due to the absence of a cap structure at the 5′ end of this pol I-promoted message.

Translational expression of *rhis4* and *rhis4-AGG* strains. Our analysis indicates that an *rhs1* (*xrn1*) mutant strain accumulates significant levels of intact and uncapped *rhis4* transcripts. It has been reported that in a number of eukaryotic organisms, certain mRNAs can be translated by a cap-independent mechanism of translation initiation (38, 45). Therefore, an important question to address is whether yeast cells also have a cap-independent mechanism of translating mRNA.

We measured the in vivo translational expression of the *rhis4* and *rhis4-AGG* transcripts in different genetic backgrounds. The level of His4 protein was quantitated relative to the level of eIF-2γ by Western blot analysis using antibodies directed against each protein. As shown in Fig. 9, the His4 protein level of the *rhis4* strain is approximately 3% that of a *HIS4*$^+$ strain (compare lanes 2 and 3). The amount of His4 protein in the

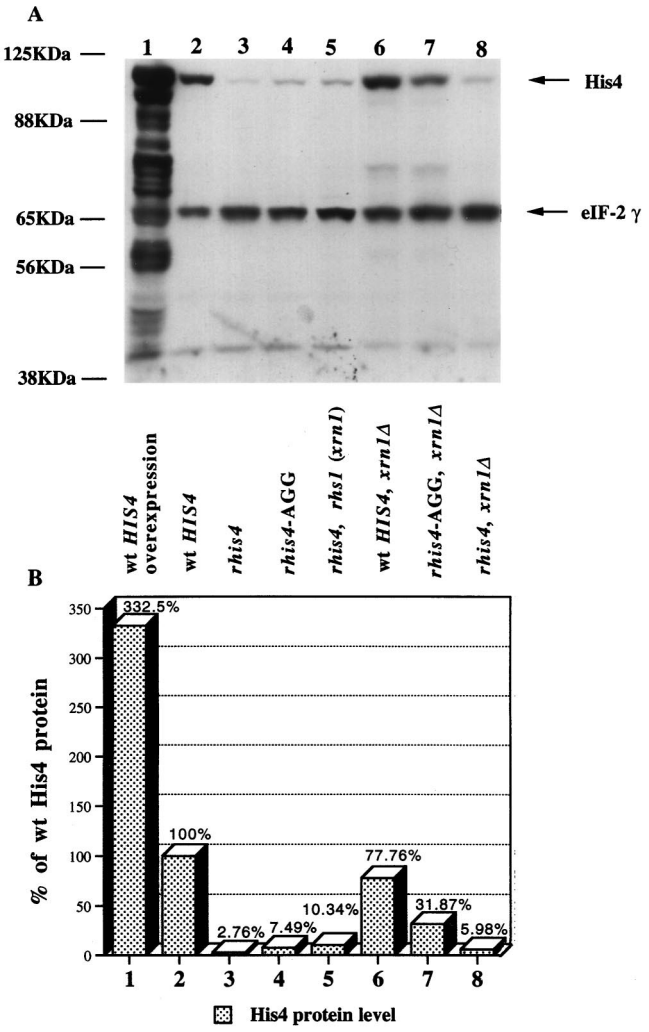

FIG. 9. Western blot analysis of the His4 protein produced in *HIS4* and *rhis4* strains. (A) Yeast crude extracts were isolated and analyzed by Western blot analysis using antibodies directed against His4 protein and antibodies directed against eIF-2γ. Crude extracts were prepared from the following yeast strains: HH879 (which contains the *HIS4*$^+$ gene on a high-copy-number YEp24 vector; lane 1); TD28 (*HIS4*$^+$; lane 2); TD237 (*rhis4*; lane 3); HJ291 (*rhis4-AGG*; lane 4); HJ35 (*rhis4 rhs1* [*xrn1*]; lane 5); HJ556 (*HIS4*$^+$ *xrn1*Δ; lane 6); HJ569 (*rhis4-AGG xrn1*Δ; lane 7); and HJ549 (*rhis4 xrn1*Δ; lane 8). (B) Bar graph illustrating the quantitation of His4 protein levels to eIF-2γ protein levels for each lane in panel A as described in Materials and Methods. The ratio of His4 protein to eIF-2γ protein levels in lane 2 represents the standard 100% level. wt, wild type.

rhis4-AGG strain is approximately 2.5-fold higher than that in the *rhis4* strain (compares 3 and 4) but only approximately 7.5% of wild-type levels (compare lanes 2 and 4). When we insert the 50-nt leader sequence derived from the rRNA portion of *rhis4-AGG* at positions −51 to −50 of the *HIS4*$^+$ leader region, we observe near wild-type levels of His4 protein (approximately 80 to 90% of wild-type levels), indicating that this sequence is not inhibitory to translation (data not shown). The finding that the level of *rhis4-AGG* mRNAs represents between 50 and 100% of wild-type *HIS4* mRNAs (Fig. 7) but the level of translation is a fraction of the wild-type protein level (7 to 8% [Fig. 9]) suggests that *rhis4-AGG* mRNAs are not translated efficiently.

This latter point is established further in Fig. 9. The amount of His4 protein measured from an *rhis4-AGG xrn1*Δ strain is approximately fourfold higher than that in the *rhis4-AGG* parent strain (compare lanes 4 and 7). However, the level of His4 protein in the *rhis4-AGG xrn1*Δ strain is only approximately 32% of that detected in a *HIS4* wild-type strain (Fig. 9; compare lanes 2 and 7) despite the level of *rhis4-AGG* mRNA being approximately 10-fold higher than that of wild-type *HIS4* mRNA (Fig. 7). This is not a result of the inability of overexpressed *HIS4* mRNA to be translated to high levels. As a control, we expressed the *HIS4* wild-type gene on a high-copy-number vector. The level of *HIS4* mRNA in this strain is approximately eightfold higher than the level of *HIS4* mRNA in the wild-type parent strain (Fig. 7; compare lanes 1 and 2). This increase is comparable to the total level of *rhis4-AGG* transcripts in an *rhs1* (*xrn1*) mutant strain. This eightfold increase in *HIS4* transcript levels results in a threefold increase in the level of intact His4 protein and an assortment of abundant, cross-reactive, and presumed proteolyzed fragments of His4 protein. Thus, the level of intact His4 protein in an *rhis4-AGG xrn1*Δ strain is only 10% of the level of intact His4 protein level (330 versus 32%) when we control for mRNA levels (Fig. 9; compare lanes 1 and 7). Judging from the abundance of proteolyzed fragments in lane 1, this 10-fold difference would appear to be grossly underestimated. Thus, the simplest explanation for the inability to see abundant His4 protein levels in an *rhis4-AGG xrn1*Δ strain is that these pol I-promoted and capless mRNAs are not efficiently translated in yeast.

DISCUSSION

Pol I-promoted uncapped *rhis4* mRNA is degraded rapidly. We have put the *HIS4* gene under the transcriptional control of pol I to generate a species of mRNA that is predominately capless in yeast. We have shown that the majority of *rhis4* transcripts is transcribed by pol I and mutations in the *XRN1* gene increases the abundance of the pol I-promoted *rhis4* mRNAs. Our analysis indicates that the *rhis4* gene produces capless mRNA that is rapidly degraded by the Xrn1, 5′-to-3′ exonuclease. Elegant studies in the Parker laboratory have mapped out the deadenylation-dependent pathway for mRNA degradation in the cytoplasm (6). The first step in degradation is deadenylation which leads to decapping and subsequent 5′-to-3′ exonucleolytic degradation of mRNA. Furthermore, it has been shown that mutations in *XRN1* lead to an increase in mRNA degradation intermediates (27). Our observations that mutations in the *xrn1* gene lead to a 9- to 10-fold increase in the combined steady-state level of *rhis4* mRNAs indicates that at least 90% of the mRNA transcribed at *rhis4* is rapidly degraded by Xrn1.

A second pathway for mRNA degradation exists in yeast commonly referred to as the nonsense-mediated decay pathway that appears to be conserved in other eukaryotic organisms (21, 46, 59). This pathway is deadenylation independent and is believed to trigger mRNA degradation as a result of a premature nonsense codon in the coding region. The fact that the level of the *rhis4-AGG* mRNA is similar to that of the *rhis4* mRNA and the amount of bicistronic *rhis4l* and *rhis4-AGGl* mRNA is not increased in a *upf1*Δ mutant argues against the *rhis4* mRNA being degraded by a nonsense-codon mediated decay pathway. The instability of the *rhis4* transcript must be due to the mRNA lacking a cap structure. This is confirmed by our immunoprecipitation analysis using anticap antibodies. Thus, our analysis confirms and extends other studies on mRNA decay in yeast which suggest that removal of the cap is the crucial step for mRNA decay and that Xrn1 is the major 5′-to-3′ exonuclease involved in decay.

3′-end formation of a pol I-promoted *rhis4* mRNA. Our analysis brings out some interesting observations on the nature of 3′-end formation of mRNA in yeast. Surprisingly, pol I-promoted *HIS4* expression produces mRNA species that terminate at the 3′ noncoding region of pol II genes. This would suggest that termination of transcription at these regions is independent of the RNA polymerase transcribing the DNA. In addition, the mRNAs produced appear to be polyadenylated based on oligo(dT) binding and PCR methodology for mapping the 3′ end of the transcript. These observations further support the notion that transcription termination at the 3′ ends of pol II genes in yeast is dictated not by a polymerase termination sequence but by polyadenylation signals (5), as the termination signals for pol I transcription are predicted to be different and presumably not present in the 3′ noncoding regions of pol II genes (35). Interestingly, the polyadenylation site for the *rhis4s* mRNA is the same as one of those for the *HIS4* mRNA (137 nt downstream of translation stop codon of *HIS4*). The polyadenylation sites for the *rhis4l* mRNA are located at the 3′ UTR of the *YCL184* gene, suggesting that it is also possible that the *rhis4l* and *YCL184* transcripts have the same polyadenylation site(s).

Considerable controversy surrounds the requirement of pol II transcription for polyadenylation. Grummt and Skinner (19) reported that pol I-promoted chloramphenicol acetyltransferase mRNAs were polyadenylated in mouse 3T6 cells. In contrast, it has been shown that pol I-promoted herpes simplex virus *tk* mRNAs were not polyadenylated in monkey COS-7 cells (53). This latter observation is more consistent with recent studies which demonstrated that the CTD of the pol II large subunit is required for efficient cleavage at the poly(A) site in vivo (39). It was also shown that the CTD might associate with CPSF and CstF but not poly(A) polymerase (39). However, our data indicate that at least in yeast, the polyadenylation machinery is able to function independently of pol II transcription. Instead, our data indicate that sequences in the 3′ noncoding region of genes, such as *HIS4* and *YCL184*, support the polyadenylation process regardless of the RNA polymerase transcribing the DNA.

Another interesting observation made in our analysis is that two transcripts accumulate as a result of pol I transcription of *HIS4*: *rhis4s* and *rhis4l*. *rhis4l* is bicistronic and presumably is a result of the inability of pol I to terminate efficiently at the 3′ end of the *HIS4* gene. One model for termination of pol II transcription in yeast is that it is an indirect consequence of nascent transcripts being polyadenylated through signals located in the 3′ noncoding region (5). Alternatively, as suggested for mammalian RNA polymerase II termination, a strong termination signal would be the combination of an efficient polyadenylation site and a strong pause site (36, 47). There are a number of possibilities as to why we observe bicistronic *rhisl* mRNA as a result of pol I transcription. One possibility is that the polyadenylation signals present at *HIS4* are not designed to promote a rate of polyadenylation coincident with the apparent higher rate of transcription associated with pol I transcription at *HIS4* (Fig. 6). Alternatively, pol I does not pause effectively in this region, and thus the mRNA structure may not always be conducive to efficient polyadenylation/termination. Either way, the *rhis4l* transcript is produced by default, at the 3′ end of *YCL184*.

The 5′ cap is required for efficient translation initiation in vivo. One of the major goals of our analysis was to determine if yeast has a cap-independent mechanism of translation initiation. The requirement for a cap in translation initiation is strongly supported by in vitro studies. Studies which have addressed the requirement for a cap in in vivo translation initiation have led to conflicting results. For example, it has been shown that the 5′ cap structure, m^7Gppp, of mature eukaryotic mRNA is required for efficient translation in microinjected oocytes (54). However, the mRNA injected lacked a poly(A) tail, which has recently been suggested to be important for translation initiation (reference 56 and references within). Grummt and Skinner (19) have shown that in mouse (3T6) cells, pol I-promoted chloramphenicol acetyltransferase mRNAs contained a poly(A) tail and were poorly expressed. However, it was not established if the mRNA lacked a 5′ cap structure. Studies of HeLa cells have shown that pol III-promoted transcripts are associated with polysomes and translated even though these transcripts were neither capped nor polyadenylated (20), which is at odds with recent models for eukaryotic translation initiation that suggest synergy between the 5′ and 3′ ends of mRNA (18, 57). Our analysis of pol I-promoted *HIS4* expression, especially in an *rhs1* (*xrn1*) or *xrn1*Δ genetic background, afforded the ability to produce a substantial level of predominantly capless mRNA that was polyadenylated. The ability of a mutation in *XRN1* to stabilize this *rhis4* mRNA strongly suggests that the mRNA is degraded in the cytoplasm, as Xrn1 is believed to be cytoplasmically located (26). Thus, *rhis4* mRNAs presumably are available to the translational machinery that is cytoplasmically located. Our analysis indicates that *rhis4-AGG* mRNA is translated at approximately 7 to 10% of the level of capped *HIS4* mRNA (Fig. 9; compare lanes 4 to 2 and lanes 7 to 1). This level may even be lower as approximately one-third of this His4 protein is still detected in an *rpa135*Δ strain (data not shown) and presumably results from translation of pol II promoted *rhis4* transcripts that are present at low level (Fig. 5). Nevertheless, quantitation of the level of His4 protein as presented here (Fig. 9) strongly indicates that pol I-promoted, capless mRNAs lack the ability to be efficiently translated in yeast and therefore suggests that a cap-dependent mechanism is preferred in yeast for efficient translation.

ACKNOWLEDGMENTS

The first two authors contributed equally to this work.

We thank T. Blumenthal, P. Cherbas, J. Jaehning, and N. Pace for helpful discussions during the course of this work. We thank J. Warner for the rDNA promoter/enhancer plasmid, M. Culbertson for the *upf1::URA3* plasmid, C. Dykstra for the *dst2* (*xrn1*)*::URA3* plasmid, C. Thompson for the pCT3 yeast genomic library, M. Nomura for the *rpa-135*Δ strains, E. Lund and R. Parker for the anticap antiserum, and R. Parker and C. Decker for advice on immunoprecipitation of mRNA with the anticap antibody.

This work was supported by Public Health Service grant GM32263 from the National Institutes of Health awarded to T.F.D.

REFERENCES

1. **Bayev, A. A., O. I. Georgiev, A. A. Hadjiolov, M. B. Kermekchiev, N. Nikolaev, K. G. Skryabin, and V. M. Zakharyev.** 1980. The structure of the yeast ribosomal genes. 2. The nucleotide sequence of the initiation site for ribosomal RNA transcription. Nucleic Acids Res. **8:**4919–4926.
2. **Beelman, C. A., and R. Parker.** 1995. Degradation of mRNA in eukaryotes. Cell **81:**179–183.
3. **Bernstein, P., and J. Ross.** 1989. Poly(A), poly(A) binding protein and the regulation of mRNA stability. Trends Biochem. Sci. **14:**373–377.
4. **Boeke, J. D., F. Lacroute, and G. R. Fink.** 1984. A positive selection of mutants lacking orotidine-5′-phosphate decarboxylase activity in yeast: 5-fluoro-orotic acid resistance. Mol. Gen. Genet. **197:**345–346.
5. **Butler, S. J., and T. Platt.** 1988. RNA processing generates the mature 3′ end of yeast *CYC1* messenger RNA *in vitro*. Science **242:**1270–1274.
6. **Caponigro, G., and R. Parker.** 1995. Multiple functions for the poly(A)-binding protein in mRNA decapping and deadenylation in yeast. Genes Dev. **9:**2421–2432.
7. **Cigan, A. M., E. K. Pabich, and T. F. Donahue.** 1988. Mutational analysis of the *HIS4* translational initiator region in *Saccharomyces cerevisiae*. Mol. Cell. Biol. **8:**2964–2975.

8. **Connelly, S., and J. L. Manley.** 1988. A functional mRNA polyadenylation signal is required for transcription termination by RNA polymerase II. Genes Dev. **2:**440–452.
9. **Conrad-Webb, H., and R. A. Butow.** 1995. A polymerase switch in the synthesis of rRNA in *Saccharomyces cerevisiae*. Mol. Cell. Biol. **15:**2420–2428.
10. **Donahue, T. F., and A. M. Cigan.** 1988. Genetic selection for mutations that reduce or abolish ribosomal recognition of the *HIS4* translational initiator region. Mol. Cell. Biol. **8:**2955–2963.
11. **Donahue, T. F., A. M. Cigan, E. K. Pabich, and B. Castilho-Valavicius.** 1988. Mutations at a Zn(II) finger motif in the yeast eIF-2b gene alter ribosomal start-site selection during the scanning process. Cell **54:**621–632.
12. **Donahue, T. F., P. J. Farabaugh, and G. R. Fink.** 1982. The nucleotide sequence of the *HIS4* region of yeast. Gene **18:**47–59.
13. **Dykstra, C. C., K. Kitada, A. B. Clark, R. K. Hamatake, and A. Sugino.** 1991. Cloning and characterization of *DST2*, the gene for DNA strand transfer protein b from *Saccharomyces cerevisiae*. Mol. Cell. Biol. **11:**2583–2592.
14. **Elion, E. A., and J. R. Warner.** 1986. An RNA polymerase I enhancer in *Saccharomyces cerevisiae*. Mol. Cell. Biol. **6:**2089–2097.
15. **Financsek, I., K. Mizumoto, Y. Mishima, and M. Muramatsu.** 1982. Human ribosomal RNA gene: nucleotide sequence of the transcription initiation region and comparison of three mammalian genes. Proc. Natl. Acad. Sci. USA **79:**3092–3096.
16. **Fresco, L. D., and S. Buratowski.** 1997. Conditional mutants of the yeast mRNA capping enzyme show that the cap enhances, but is not required for, mRNA splicing. RNA **2:**584–596.
17. **Frohman, M. A.** 1993. Rapid amplification of complementary DNA ends for generation of full-length complementary DNAs: thermal RACE. Methods Enzymol. **218:**340–356.
18. **Gallie, D. R.** 1991. The cap and poly(A) tail function synergistically to regulate mRNA translational efficiency. Genes Dev. **5:**2108–2116.
19. **Grummt, I., and J. A. Skinner.** 1985. Efficient transcription of a protein-coding gene from the RNA polymerase I promoter in transfected cells. Proc. Natl. Acad. Sci. USA **82:**722–726.
20. **Gunnery, S., and M. B. Mathews.** 1995. Functional mRNA can be generated by RNA polymerase III. Mol. Cell. Biol. **15:**3597–3607.
21. **Hagan, K. W., M. J. Ruiz-Echevarria, Y. Quan, and A. W. Peltz.** 1995. Characterization of *cis*-acting sequences and decay intermediates involved in nonsense-mediated mRNA turnover. Mol. Cell. Biol. **15:**809–823.
22. **Hagler, J., and S. Shuman.** 1992. A freeze-frameview of eukaryotic transcription during elongation and capping of nascent mRNA. Science **255:**983–986.
23. **Hamm, J., and I. W. Mattaj.** 1990. Monomethylated cap structures facilitate RNA export from the nucleus. Cell **63:**109–118.
24. **Heidmann, S., B. Obermaier, K. Vogel, and H. Domdey.** 1992. Identification of pre-mRNA polyadenylation sites in *Saccharomyces cerevisiae*. Mol. Cell. Biol. **12:**4215–4229.
25. **Hershey, J. W. B.** 1991. Translational control in mammalian cells. Annu. Rev. Biochem. **60:**717–755.
26. **Heyer, W.-D., A. W. Johnson, U. Reinhart, and R. D. Kolodner.** 1995. Regulation and intracellular localization of *Saccharomyces cerevisiae* strand exchange protein (*Sep1*/*Xrn1*/*Kem1*), a multifunctional exonuclease. Mol. Cell. Biol. **15:**2728–2736.
27. **Hsu, C. L., and A. Stevens.** 1993. Yeast cells lacking 5′→3′ exoribonuclease 1 contain mRNA species that are poly(A) deficient and partially lack the 5′ cap structure. Mol. Cell. Biol. **13:**4826–4835.
28. **Huang, H-K., H.-J. Lo, and T. F. Donahue.** Unpublished data.
29. **Huang, H-K., H. Yoon, E. M. Hannig, and T. F. Donahue.** 1997. GTP hydrolysis controls stringent selection of the AUG start codon during translation initiation in *Saccharomyces cerevisiae*. Genes Dev. **11:**2396–2413.
30. **Izaurralde, E., J. Lewis, C. McGuigan, M. Jankowska, E. Darzynkiewicz, and I. W. Mattaj.** 1994. A nuclear cap binding protein complex involved in pre-mRNA splicing. Cell **78:**657–668.
31. **Jacobson, A., and M. Favreau.** 1983. Possible involvement of poly(A) in protein synthesis. Nucleic Acids Res. **18:**6353–6368.
32. **Jove, R., and J. L. Manley.** 1982. Transcription initiation by RNA polymerase II is inhibited by S-adenosylhomocysteine. Proc. Natl. Acad. Sci. USA **79:**5842–5846.
33. **Klemenz, R., and E. P. Geiduschek.** 1980. The 5′ terminus of the precursor ribosomal RNA of *Saccharomyces cerevisiae*. Nucleic Acids Res. **8:**2679–2689.
34. **Kozak, M.** 1989. The scanning model for translation: an update. J. Cell Biol. **108:**229–241.
35. **Lang, W., and R. H. Reeder.** 1993. The REB1 site is an essential component of a terminator for RNA polymerase I in *Saccharomyces cerevisiae*. Mol. Cell. Biol. **13:**649–658.
36. **Lanoix, J., and N. H. Acheson.** 1988. A rabbit β-globin polyadenylation signal directs efficient termination of transcription of polyomavirus DNA. EMBO J. **7:**2515–2522.
37. **Long, E. O., M. L. Rebbert, and I. B. Dawid.** 1981. Nucleotide sequence of the initiation site for ribosomal RNA transcription in *Drosophila melanogaster*: comparison of genes with and without insertions. Proc. Natl. Acad. Sci. USA **78:**1513–1517.
38. **Macejak, D. G., and P. Sarnow.** 1991. Internal initiation of translation mediated by the 5′ leader of a cellular mRNA. Nature **353:**90–94.
39. **McCracken, S., N. Fong, K. Yankulov, S. Ballantyne, G. Pan, J. Greenblatt, S. D. Patterson, M. Wickens, and D. L. Bentley.** 1997. The C-terminal domain of RNA polymerase II couples mRNA processing to transcription. Nature **385:**357–361.
40. **Muhlrad, D., C. J. Decker, and R. Parker.** 1994. Deadenylation of the unstable mRNA encoded by the yeast *MFA2* gene leads to decapping followed by 5′ to 3′ digestion of the transcript. Genes Dev. **8:**855–866.
41. **Muhlrad, D., C. J. Decker, and R. Parker.** 1995. Turnover mechanisms of the stable yeast *PGK1* mRNA. Mol. Cell. Biol. **15:**2145–2156.
42. **Munns, T. W., M. K. Liszewski, J. T. Tellam, H. F. Sims, and R. E. Rhoads.** 1982. Antibody-nucleic acid complexes. Immunospecific retention of globin messenger ribonucleic acid with antibodies specific for 7-methyl guanosine. Biochemistry **21:**2922–2928.
43. **Nagawa, F., and G. R. Fink.** 1985. The relationship between the "TATA" sequence and transcription initiation sites at the *HIS4* gene of *Saccharomyces cerevisiae*. Proc. Natl. Acad. Sci. USA **82:**8557–8561.
44. **Nogi, Y., R. Yano, and M. Nomura.** 1991. Synthesis of large rRNAs by RNA polymerase II in mutants of *Saccharomyces cerevisiae* defective in RNA polymerase I. Proc. Natl. Acad. Sci. USA **88:**3962–3966.
45. **Oh, S. K., M. P. Scott, and P. Sarnow.** 1992. Homeotic gene *Antennapedia* mRNA contains 5′ noncoding sequences that confer translational initiation by internal ribosome binding. Genes Dev. **6:**1643–1653.
46. **Peltz, S. W., J. L. Donahue, and A. Jacobson.** 1992. A mutation in the tRNA nucleotidyltransferase gene promotes stabilization of mRNAs in *Saccharomyces cerevisiae*. Mol. Cell. Biol. **12:**5778–5784.
47. **Proudfoot, N. J.** 1989. How RNA polymerase II terminates transcription in higher eukaryotes. Trends Biol. Sci. **14:**105–110.
48. **Rad, M. R., K. Lutzenkirchen, G. Xu, U. Kleinhans, and C. P. Hollenberg.** 1991. The complete sequence of a 11,953 bp fragment from C1G on chromosome III encompasses four new open reading frames. Yeast **7:**533–538.
49. **Rasmussen, E. B., and J. T. Lis.** 1993. In vivo transcriptional pausing and cap formation on three Drosophila heat shock genes. Proc. Natl. Acad. Sci. USA **90:**7923–7927.
50. **Sachs, A. B., and R. W. Davis.** 1990. Translation initiation and ribosomal biogenesis: involvement of a putitive RNA helicase and RPL46. Science **247:**1077–1079.
51. **Sambrook, J., E. F. Fritsch, and T. Maniatis.** 1989. Molecular cloning: a laboratory manual, 2nd ed. Cold Spring Harbor Laboratory, Cold Spring Harbor, N.Y.
52. **Sherman, F., G. R. Fink, and C. W. Lawrance.** 1972. Methods in yeast genetics. Cold Spring Harbor Laboratory, Cold Spring Harbor, N.Y.
53. **Smale, S. T., and R. Tjian.** 1985. Transcription of herpes simplex virus *tk* sequences under the control of wild-type and mutant human RNA polymerase I promoters. Mol. Cell. Biol. **5:**352–362.
54. **Sonenberg, N.** 1988. Cap-binding proteins of eukaryotic messenger RNA: functions in initiation and control of translation. Prog. Nucleic Acid Res. Mol. Biol. **35:**173–207.
55. **Sonenberg, N.** 1990. Poliovirus translation. Curr. Top. Microbiol. Immunol. **161:**23–47.
56. **Tarun, S. Z., Jr., and A. B. Sachs.** 1995. A common function for mRNA 5′ and 3′ ends in translation initiation in yeast. Genes Dev. **9:**2997–3007.
57. **Tarun, S. Z., Jr., and A. B. Sachs.** 1996. Association of the yeast poly(A) binding protein with translation initiation factor eIF-4G. EMBO J. **15:**7168–7177.
58. **Wickens, M.** 1990. How the messenger got its tail: addition of poly(A) in the nucleus. Trends Biochem. Sci. **15:**277–281.
59. **Wisdom, R., and W. Lee.** 1990. Translation of *c-myc* mRNA is required for its post-transcriptional regulation during myogenesis. J. Biol. Chem. **265:**19015–19021.
60. **Yano, R., and M. Nomura.** 1991. Suppressor analysis of temperature-sensitive mutations of the largest subunit of RNA polymerase I in *Saccharomyces cerevisiae*: a suppressor gene encodes the second-largest subunit of RNA polymerase I. Mol. Cell. Biol. **11:**754–764.